Published in final edited form as:

Biochemistry. 2019 May 28; 58(21): 2534–2541. doi:10.1021/acs.biochem.9b00297.

Mechanism of the Flavoprotein D-6-Hydroxynicotine Oxidase: Substrate Specificity, pH and Solvent Isotope Effects, and Roles of Key Active-Site Residues

Paul F. Fitzpatrick[*,†], **Vi Dougherty**[†], **Bishnu Subedi**[†], **Jesus Quilantan**[†], **Cynthia S. Hinck**[†], **Andreina I. Lujan**[†], **Jose R. Tormos**[‡]

[†]Department of Biochemistry and Structural Biology, University of Texas Health Science Center, San Antonio, Texas 78229, United States

[‡]Department of Chemistry, St. Mary's University, San Antonio, Texas 78228, United States

Abstract

The flavoprotein D-6-hydroxynicotine oxidase catalyzes an early step in the oxidation of (*R*)-nicotine, the oxidation of a carbon–nitrogen bond in the pyrrolidine ring of (*R*)-6-hydroxynicotine. The enzyme is a member of the vanillyl alcohol oxidase/*p*-cresol methylhydroxylase family of flavoproteins. The effects of substrate modifications on the steady-state and rapid-reaction kinetic parameters are not consistent with the quinone-methide mechanism of *p*-cresol methylhydroxylase. There is no solvent isotope effect on the k_{cat}/K_{amine} value with either (*R*)-6-hydroxynicotine or the slower substrate (*R*)-6-hydroxynornicotine. The effect of pH on the rapid-reaction kinetic parameters establishes that only the neutral form of the substrate and the correctly protonated form of the enzyme bind. The active-site residues Lys348, Glu350, and Glu352 are all properly positioned for substrate binding. The K348M substitution has only a small effect on the kinetic parameters; the E350A and E350Q substitutions decrease the k_{cat}/K_{amine} value by ~20- and ~220-fold, respectively, and the E352Q substitution decreases this parameter ~3800-fold. The k_{cat}/K_{amine}–pH profile is bell-shaped. The pK_a values in that profile are altered by replacement of (*R*)-6-hydroxynicotine with (*R*)-6-hydroxynornicotine as the substrate and by the substitutions for Glu350 and Glu352, although the profiles remain bell-shaped. The results are consistent with a network of hydrogen-bonded residues in the active site being involved in binding the neutral form of the amine substrate, followed by the transfer of a hydride from the amine to the flavin.

Graphical Abstract

[*]**Corresponding Author**: Department of Biochemistry and Structural Biology, University of Texas Health Science Center, San Antonio, TX 78229. fitzpatrickp@uthscsa.edu. Phone: (210) 567-8264.

Supporting Information

The Supporting Information is available free of charge on the ACS Publications website at DOI: 10.1021/acs.biochem.9b00297. Effect of substrate concentration on the apparent first-order rate constant for reduction (Figure S1), effect of pH on the limiting rate constant for reduction and the K_d value (Figure S2), effect of pD on the k_{cat}/K_m value (Figure S3), and alternative fits for the k_{cat}/K_{amine}–pH profile with (*R*)-6-hydroxynicotine as the substrate (Figure S4) (PDF)

Accession Codes

The UniProtKB accession ID for DHNO from *A. nicotinovorans* is Q8GAG1.

The authors declare no competing financial interest.

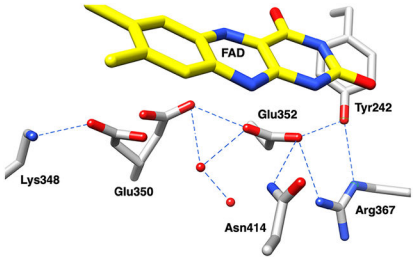

There are two major microbial pathways for degradation of the plant alkaloid nicotine.[1,2] In the pathway best characterized in *Pseudomonas putida*,[3] the initial step is the oxidation of the pyrrolidine ring of (S)-nicotine to form *N*-methyl-myosmine catalyzed by the flavoprotein nicotine oxidase.[4,5] In the pathway best characterized in *Arthrobacter*,[1,6] the initial step is the hydroxylation of the pyridyl ring by the molybdopterin enzyme nicotine dehydrogenase,[7] which is active on both (*S*)- and (*R*)-nicotine. The pyrrolidine ring of the resulting 6-hydroxynicotine is then oxidized by either L- or D-6-hydroxynicotine oxidase to form 6-hydroxy-*N*-methylmyosmine.[8,9] The structures of these two flavoproteins[10,11] and of nicotine oxidase[5] establish that L-6-hydroxynicotine oxidase (LHNO) and nicotine oxidase are members of the monoamine oxidase family of flavoproteins,[12] while D-6-hydroxynicotine oxidase (DHNO) is a member of the vanillyl alcohol oxidase/*p*-cresol methylhydroxylase (VAO/PCMH) family.[13]

Initial characterization of the products of the reactions catalyzed by DHNO and LHNO in the 1960s identified the common product of both reactions, 6-hydroxy-*N*-methylmyosmine, as resulting from oxidation of a carbon–carbon bond in the pyrrolidine ring of the substrate.[9,14] In light of this, the finding that DHNO is a member of the VAO/PCMH family led Koetter and Schultz[10] to propose the mechanism in Scheme 1 for this enzyme on the basis of the proposed involvement of a quinone methide intermediate in the vanillyl alcohol oxidase reaction.[15] They also proposed explicit roles for several active-site residues. However, it has recently been established that LHNO and DHNO do not catalyze oxidation of the pyrrolidine C1′–C2′ bond but rather the C1′–N bond.[16,17] In addition, the VAO/PCMH family is quite diverse, with many members catalyzing reactions unlikely to involve a quinone methide intermediate.[13] The work presented here describes the results of experiments designed to evaluate the mechanism in Scheme 1 for DHNO.

EXPERIMENTAL PROCEDURES

Materials.

(*R,S*)-6-Hydroxynicotine was from Princeton Biomolecular Research. (*R*)-6-Hydroxynornicotine was from NetChem, Inc. (*R,S*)-4-(1-Methylpyrrolidine-2-yl)phenol was from Aurora Fine Chemicals LLC (San Diego, CA). Other chemicals, including (*R*)-nicotine and (*R,S*)-6-chloronicotine, were purchased from Sigma-Aldrich or ThermoFisher.

Protein Expression and Purification.

A synthetic gene for wild-type DHNO from *Arthrobacter nicotinovorans* optimized for expression in *Escherichia coli* was obtained from DNA2.0. This was subcloned into the

*Nco*I/*Bam*HI restriction sites of pET-23d(+) (Novagen) for expression of the protein with an N-terminal six-His tag. Mutations were generated using the QuikChange II Site-Directed Mutagenesis Kit (Agilent Technologies) with primers designed for the specific mutations (Integrated DNA Technologies, Inc.). In all cases, the sequences of the resulting plasmids were confirmed by DNA sequencing (GenScript). The resulting plasmids were used to transform *E. coli* BL21(DE3) containing the pGro7 chaperone plasmid (Takara Bio, Inc.). For protein purification, 1 L of LB medium with 50 μg/mL ampicillin, 20 μg/mL chloramphenicol, and 0.5 mg/mL arabinose was inoculated with 10 mL of an overnight culture of the same medium inoculated with a single colony. The cells were grown at 37 °C until the A_{600} reached ~0.7, at which point they were cooled to 18 °C. Protein expression was then induced using 0.5 mM isopropyl β-D-1-thiogalactopyranoside. After growing overnight at 18 °C, cells were harvested by centrifugation (6200g, 15 min, 4 °C), and the cell paste was resuspended in 50 mM Na-HEPES (pH 8.0), 0.1 M NaCl, and 10 mM imidazole, using 8 mL/g of cell paste. After the addition of lysozyme (100 μg/mL), leupeptin (2 μM), and pepstatin A (2 μM), the solution was stirred at 4 °C for 15 min. The cells were lysed by sonication for 5 min using a Branson Sonifier 450 at a 50% duty cycle and a total output level of 5. The lysate was then centrifuged (27000g, 30 min, 4 °C) to remove cell debris. Solid streptomycin sulfate was added to a final concentration of 1.5% at 4 °C. After centrifugation (27000g, 30 min, 4 °C) to remove precipitated nucleic acids, the supernatant was loaded onto a 5 mL HisTrap FF Crude column (GE Healthcare) equilibrated with 50 mM HEPES (pH 8.0), 0.1 M NaCl, and 10 mM imidazole. The column was washed with the same buffer until the conductivity stabilized, and the protein was eluted using a gradient from 10 to 100 mM imidazole in 100 mL of the same buffer. Fractions containing DHNO were identified by polyacrylamide gel electrophoresis in the presence of sodium dodecyl sulfate, pooled, and concentrated using an Amicon Stirred Cell and an Ultra-15 10K centrifugal filter (EMD Millipore). The sample was then loaded onto a 120 mL HiLoad Superdex 200 prep grade column (GE Healthcare) in 50 mM HEPES (pH 8.0) and 0.1 M NaCl. Fractions containing DHNO were pooled and dialyzed into 50 mM HEPES (pH 8.0), 0.1 M NaCl, and 10 mM dithiothreitol, with two buffer changes. The resulting purified protein was stored at −80 °C. The concentration of DHNO was determined from the flavin visible absorbance spectrum using an ε_{453} value of 11300 M^{-1} cm^{-1} and a molecular mass of 49 kDa.

Assays.

The activity of DHNO was determined using a Yellow Springs Instruments model 5300A oxygen electrode to follow oxygen consumption. Standard assays were performed in 0.1 HEPES (pH 8.0) and 0.1 M NaCl at 25 °C using ~0.1 μM enzyme. The concentration of oxygen was varied by bubbling the desired concentration of oxygen (62 μM to 1.25 mM) into the oxygen electrode cell for ~10 min. Values of k_{cat}/K_{amine} were determined by varying the concentration of the amine from ~10% to at least 5 times the K_m value in air-saturated buffer (250 μM oxygen). Values of k_{cat} and k_{cat}/K_{O_2} were determined by varying the concentration of oxygen (60 μM to 1.2 mM) at a high concentration of the amine (1–4 mM). For analyses of pH effects, the buffers were 0.1 M Na-HEPES for pH 7–8.25, 0.1 M Na-CHES for pH 8.5–10.5, and 0.1 M Na-CAPS for pH 10–11. The concentration of the

enzyme varied from 0.1 to 1 μM. Anaerobic stopped-flow analyses monitored the change in the flavin spectrum at 450 nm and utilized 10–50 μM enzyme. Anaerobic conditions were achieved as previously described.[18]

Data Analysis.

k_{cat}, K_m, and k_{cat}/K_m values were determined by fitting initial rate data to the Michaelis–Menten equation. When racemic substrates were used, it was assumed that only the *R* isomer was a substrate for DHNO and that the racemic compounds contained equimolar amounts of the two stereoisomers. Apparent first-order rate constants for reduction of DHNO were determined using eq 1

$$A_t = A_\infty + \Delta A e^{-k_{obs}t} \quad (1)$$

which describes a monophasic exponential decrease in which ΔA is the absorbance change, k_{obs} is the apparent first-order rate constant, and A_∞ is the absorbance of the fully reduced enzyme. The k_{red} and K_d values were determined from the k_{obs} values at each concentration of substrate using eq 2.[19]

$$k_{obs} = S \times k_{red}/(K_d + S) \quad (2)$$

The pH dependence of the k_{cat}/K_{amine} values was analyzed using eq 3

$$\log Y = \log \frac{c}{1 + \frac{H}{K_1} + \frac{K_2}{H}} \quad (3)$$

which describes the pH behavior of a kinetic parameter (*Y*) that decreases from a constant value (*c*) at both high and low pH. The program KaleidaGraph (Synergy Software) was used for fitting. The error bars in the individual values in figures are smaller than the size of the symbols if no errors are indicated. The steady-state kinetic data at pH 8 for the wild-type enzyme and variants have been deposited in Strenda DB as entry MID 13401.

RESULTS

Steady-State Kinetics.

In essentially all cases examined to date, the kinetic mechanism for flavoprotein oxidases involves reaction of the substrate with the enzyme to form the oxidized substrate and reduced enzyme; the reduced enzyme then reacts with molecular oxygen to form the oxidized enzyme, with release of the oxidized amine as the last step (Scheme S1).[20,21] This results in the enzyme kinetics fitting to a ping-pong kinetic equation (eq 4), so that the k_{cat}/K_m values for the substrates are independent of the concentration of the other substrate. That this was the case for DHNO was confirmed by varying the concentration of (*R*)-6-

hydroxynicotine and oxygen in a fixed ratio.[22] In the case of data fitting well to eq 1, such an experiment will yield a plot of the initial rate versus the concentration of either substrate that fits well to the Michaelis–Menten equation. In contrast, for data fitting better to the more complex equation for a sequential mechanism, the additional term in the equation results in a poor fit to the Michaelis–Menten equation and requires additional terms involving the square of the substrate concentration. When the concentrations of (*R*)-6-hydroxynicotine and oxygen were varied in a 1:1 ratio, the effect of the substrate concentration on the initial velocity was described well by the Michaelis–Menten equation (results not shown), establishing that the steady-state kinetics for DHNO can be described by eq 4. Consequently, intrinsic k_{cat}/K_m values for the oxidized substrate can be determined at any concentration of oxygen, greatly simplifying their measurement.

$$\frac{v}{e} = \frac{k_{cat}[\text{amine}][O_2]}{[\text{amine}][O_2] + K_{\text{amine}}[O_2] + K_{O_2}[\text{amine}]} \quad (4)$$

Table 1 gives the steady-state kinetic parameters at pH 8 for DHNO with (*R*)-6-hydroxynicotine and several analogues (Scheme 2). For the physiological substrate, the kinetics were examined by varying the concentrations of both the amine and oxygen. This yielded a K_{O_2} value several-fold higher than the solubility of oxygen at 25 °C of 1.2 mM, so that the k_{cat} and K_m values may be underestimated. However, the more relevant k_{cat}/K_m values are unaffected by this. In the case of the analogues, initial rates were determined in air-saturated buffer to obtain the intrinsic k_{cat}/K_{amine} values, the usual criterion for substrate specificity, but only apparent k_{cat} and K_{amine} values. Loss of the methyl group (6-hydroxynornicotine) decreases the k_{cat}/K_{amine} value ~16-fold. Replacing the oxygen atom with chlorine (6-chloronicotine) or the pyridyl ring with a phenyl ring [4-(1-methylpyrrolidine-2-yl)phenol] results in a decrease of 100-fold. The effect of removing both the methyl group and the oxygen (nicotine) is an ~2500-fold decrease, approximately equivalent to the combination of the separate effects of these two modifications.

Rapid-Reaction Kinetics.

The kinetics of reduction of DHNO were determined by following the decrease in the visible absorbance of the FAD cofactor in the absence of oxygen. With all of the substrates examined, the reactions could be fit as a single exponential (eq 1). The values for the limiting rate constant for flavin reduction, k_{red}, and the apparent K_d were determined by fitting the values of the observed rate constants for reduction as a function of amine concentration to eq 2 (Figure S1). The effects of substrate modifications on the value of k_{red} generally parallel the effects on the k_{cat}/K_{amine} value (Table 2). The K_d values for (*R*)-6-chloronicotine and (*R*)-4-(1-methylpyrrolidine-2-yl)phenol are effectively the same as that for (*R*)-6-hydroxynicotine, while that for (*R*)-6-hydroxynornicotine is ~5-fold higher and that for (*R*)-nicotine ~10-fold lower.

pH Effects.

To gain insight into the required protonation states of the substrates and active-site residues, the effects of pH on the k_{cat}/K_{amine} values for both (*R*)-6-hydroxynicotine and (*R*)-6-hydroxynornicotine were determined for wild-type DHNO. As shown in Figure 1A, the two profiles showed decreases at both high and low pH, consistent with a single residue that must be protonated for efficient catalysis and a single residue that must be unprotonated. Fitting the data to eq 3 yielded the individual pK_a values. The pK_a values from the (*R*)-6-hydroxynicotine profile are both ~0.5 less than the pK_a values from the (*R*)-6-hydroxynornicotine profile (Table 3). In contrast to the effects of pH on the k_{cat}/K_{amine} value, the value of k_{red} with (*R*)-6-hydroxynicotine as the substrate is unaffected by pH between pH 7 and 10 (Figure S2A). The pH dependence of the K_a value for (*R*)-6-hydroxynicotine matches that of the k_{cat}/K_{amine} value, a bell-shaped profile with an optimum of pH 8.0 and poorly separated pK_a values (Figure S2B).

Solvent Isotope Effects.

Solvent isotope effects on the k_{cat}/K_{amine} value were measured to determine whether any solvent-exchangeable protons are in flight during kinetically significant steps during oxidation of the amine substrate. With (*R*)-6-hydroxynicotine as the substrate in D_2O, the pD dependence of this kinetic parameter is still described well by eq 3, but the optimum shifts to pD 8.5 (Figure S3A). The ratio of the pL-dependent maxima for the fits of the k_{cat}/K_{amine} pH and pD profiles yields a solvent isotope effect on the k_{cat}/K_{amine} value of 1.1 ± 0.5. To improve the precision of this value, the k_{cat}/K_{amine} value was determined at pH 8 and pD 8.5 in a single experiment; this gave a solvent isotope effect on the k_{cat}/K_{amine} value for (*R*)-6-hydroxynicotine of 1.04 ± 0.10. The k_{cat}/K_{amine} value with (*R*)-6-hydroxynornicotine as a substrate shows a similar shift in the pK_a values in D_2O (Figure S3B). Comparison of the pL-dependent maxima of the k_{cat}/K_{amine} value from the two pL profiles gives a solvent isotope effect on the k_{cat}/K_{amine} value with (*R*)-6-hydroxynornicotine of 0.88 ± 0.15.

Mutagenesis of Active-Site Residues.

In the mechanism shown in Scheme 1, the active-site residues Lys348, Glu350, and Glu352 are all involved in oxidation of the amine. Consequently, the effect of substituting these three residues on the activity of the enzyme was examined. Glu350 and Glu352 were both replaced by glutamine to eliminate the ability to act as an active-site acid or base but retain the ability to form a hydrogen bond; Glu350 was also replaced with alanine to eliminate both potential roles. Lys348 was mutated to methionine to remove the positive charge and similarly eliminate the potential involvement in proton transfer. The steady-state kinetic parameters of these variants with (*R*)-6-hydroxynicotine as the substrate are listed in Table 1. The K348M substitution has the smallest effect, with a decrease in the k_{cat}/K_{amine} value of only 2–3-fold and a small decrease in the k_{cat} value. Similar decreases in the k_{cat}/K_{amine} and k_{cat} values occur with (*R*)-6-hydroxynornicotine as the substrate for this variant. The E350Q substitution results in a much larger decrease of ~200-fold in the k_{cat}/K_{amine} value with (*R*)-6-hydroxynicotine and an 8-fold decrease in the k_{cat} value. The E350A substitution has a smaller effect than the E350Q substitution, with the k_{cat}/K_{amine} value for (*R*)-6-

hydroxynicotine down only 20-fold from the wild-type value and the k_{cat} value down ~4-fold. Finally, the E352Q substitution has the largest effect, with decreases of ~4000- and ~100-fold in the k_{cat}/K_{amine} and k_{cat} values for (*R*)-6-hydroxynicotine, respectively. The effects on the k_{red} value are similar, with the K348M substitution having only a small effect and the E352Q mutation having the largest effect. Again, the E350A variant is more active than the E350Q enzyme, with a k_{red} value that is ~70% of the wild-type value. The E350A, E350Q, and E352Q substitutions all result in large increases (10–60-fold) in the K_d value for (*R*)-6-hydroxynicotine. The k_{cat}/K_{O_2} value is affected much less by the substitutions, with all but the E352Q variant having a value within 2-fold of the wild-type value. Even for this lowest-activity variant, the k_{cat}/K_{O_2} value is down only 5-fold, far less than the decrease seen in the k_{cat}/K_{amine} value.

Because all of the substitutions involved ionizable residues, the effects of pH on the k_{cat}/K_{amine} value with (*R*)-6-hydroxynicotine were determined for each variant (Table 3 and Figure 1B). In all cases, the profiles are bell-shaped. Fitting the data for K248M DHNO to eq 3 yields reversed pK_a values, with pK_1 > pK_2. Because the individual pK_a values cannot be resolved in such a case, the data were analyzed using eq 1 with pK_1 being equal to pK_2 to obtain an average pK_a value of 8.2. This is essentially the same as the average of the pK_a values for the wild-type enzyme. A similar analysis of the data for the wild-type enzyme results in a slight increase in the X^2 value from 0.391 to 0.519 but a visually indistinguishable plot (Figure S4). The effect of pH on the k_{cat}/K_{amine} profile with (*R*)-6-hydroxynornicotine was also determined for K248M DHNO; the two pK_a values are better resolved with this substrate and unchanged from the values for the wild-type enzyme (Table 3). With (*R*)-6-hydroxynicotine as the substrate, the E350Q and E350A variants have identical pK_a values; these show much greater separation than is seen with the wild-type enzyme due to the pK_a value for the group that must be protonated increasing to ~9.7 for both variants. Finally, with the E352Q variant, both pK_a values are pushed farther from neutrality; both values have less than ideal precision due to the low activity of this variant and its instability at pH extremes.

DISCUSSION

In the absence of prior mechanistic studies of DHNO, the finding that its structure places the enzyme in the same structural family of flavoproteins as *p*-cresol methylhydroxylase suggested that the two enzymes have a common mechanism involving a quinone methide intermediate (Scheme 1).[10] While this mechanism was based on the pyridinol tautomer rather than the more likely pyridinone[23] as the substrate and on the incorrect identification of the reaction product,[16] it can readily be modified to accommodate these issues. The mechanism of Scheme 3 is based on the mechanism proposed for oxidation of hydroxybenzylamines by vanillyl alcohol oxidase[24] and is consistent with the structural data. However, in the decade or so since the structure of DHNO was determined, a great deal more has been learned about the VAO/PCMH family.[13] This family catalyzes a range of alcohol and amine oxidations that do not involve *p*-quinone methide intermediates. Indeed, one of the closest structural homologues of DHNO is tirandamycin oxidase, which catalyzes

oxidation of a secondary alcohol.[25] The mechanism of that enzyme is proposed to involve direct transfer of a hydride to the flavin as the alcohol proton is accepted by a tyrosine residue, a mechanism similar to that of flavoprotein alcohol oxidases belonging to other structural families.[26–29] Most flavoproteins that oxidize amines do so by direct oxidation of the carbon–nitrogen bond, transferring a hydride to the flavin cofactor from the neutral amine.[21] Indeed, this is the mechanism that has been proposed for cytokinin dehydrogenase, another member of the VAO/PCMH family.[30] Thus, the identification of DHNO as a member of this family is also consistent with the minimal mechanism in Scheme 4.

The steady-state and rapid-reaction kinetic data for DHNO are consistent with the kinetic mechanism for the enzyme being that typically seen with flavoprotein oxidases, oxidation of the amine and reduction of the flavin in the first half-reaction, followed by reaction of the reduced flavin with oxygen to regenerate the oxidized enzyme–product complex.[21] Because the rate constant for flavin reduction, k_{red}, is significantly greater than the k_{cat} for the wild-type and mutant enzymes with the natural substrate, release of the product from the oxidized enzyme is the likely rate-determining step under k_{cat} conditions (Scheme S1). Therefore, the most informative kinetic parameter for understanding the mechanism of DHNO is k_{cat}/K_{amine}, which reflects the reaction of the free enzyme and the free amine substrate through oxidation of the substrate. The k_{red} value provides a direct measure of the rate constant for amine oxidation

The kinetics of 6-hydroxynicotine analogues provide insight into the structural features of the substrate that determine reactivity. On the basis of the k_{cat}/K_{amine} values in Table 1 and the rapid-reaction parameters in Table 2, the pyridinone ring is key to the substrate specificity, with the methyl moiety playing a smaller role. Removal of the latter to form (*R*)-4-hydroxynornicotine decreases the k_{cat}/K_{amine} value by 16-fold; this can be partitioned equally between decreases of 4-fold in the K_d and k_{red} values. Both (*R*)-6-chloronicotine and (*R*)-4-(1-methylpyrrolidine-2-yl)phenol are isosteric with (*R*)-6-hydroxynicotine; however, the pyridyl tautomer is predominant rather than the pyridinone for 6-chloronicotine, and 4-(1-methylpyrrolidine-2-yl)phenol is an analogue for the former. The k_{cat}/K_{amine} values for both are ~100-fold lower than the value for the native substrate, and this decrease is reflected in comparable decreases in the k_{red} value. The decrease with (*R*)-4-(1-methylpyrrolidine-2-yl)phenol is much greater than one would expect if the mechanism of Scheme 1 were correct, while the decrease seen with (*R*)-6-chloronicotine is larger than the mechanism of Scheme 3 predicts. (*R*)-Nicotine is the slowest substrate examined here, consistent with a combination of the effects of the loss of the methyl group and the predominance of its pyridyl tautomer.

In the mechanisms in both Schemes 1 and 3, a solvent-exchangeable proton is in flight as the hydride is transferred to the flavin, while this is not the case in the mechanism of Scheme 4. Any such proton transfer should result in a solvent isotope effect on the k_{cat}/K_m value for the amine substrate, but there is no effect with either (*R*)-6-hydroxynicotine or (*R*)-6-hydroxynornicotine. Kinetic isotope effects on k_{cat}/K_m values can be suppressed if the rate constant for the chemical step is comparable to or larger than the rate constant for substrate dissociation, resulting in a high commitment to catalysis.[31] This is less of a problem with slower substrates, because these exhibit reduced rate constants for catalysis. The lack of a

solvent isotope effect with the native substrate for DHNO could be attributed to such an effect, but the similar result with the slower substrate (*R*)-6-hydroxynornicotine makes it much less likely that a commitment is suppressing a solvent isotope effect. Thus, the lack of a solvent isotope effect is more consistent with the mechanism of Scheme 4 than those in Schemes 1 and 3, supporting the conclusion drawn from the analysis of substrate specificity.

Lys348, Glu350, and Glu352 were selected for mutagenesis on the basis of the proposal by Koetter and Schulz that they bind the substrate (Scheme 1).[10] In the absence of any structure of the enzyme with a ligand bound, the exact mode of substrate binding in DHNO is unclear. Indeed, Heath et al.[16] have separately proposed a model for binding of the substrate to DHNO in which Glu350 and Glu352 both bind the substrate but Lys348 has no role. In our hands, (*R*)-6-hydroxynicotine is readily modeled into the active site with its C1′ 3.8–4 Å from flavin N5, the appropriate position for hydride transfer, but several arrangements are possible for the interactions with the two glutamate residues (results not shown). In addition, the structure of DHNO shows the side chain of Glu350 in two different positions with equal occupancies (Figure 2).[10] In one, a carboxylate oxygen of Glu350 is an appropriate distance for a hydrogen bond (2.8 Å in one subunit and 3.1 Å in the other) from a carboxylate oxygen of Glu352; in the other orientation, the other carboxylate oxygen of Glu350 is 2.7 Å from the side chain nitrogen of Lys348 in one of the two subunits. This introduces further uncertainty into the results of any docking.

Mutagenesis of Lys348 to methionine results in relatively small decreases in the k_{cat}/K_{amine} (2–3-fold) and k_{red} (~35%) values at pH 8. This small effect and the lack of a solvent isotope effect rule out a role for this residue as accepting a proton from the substrate during catalysis and suggest that this residue might not interact directly with the substrate at all. The small changes in the kinetic parameters that result from this mutation are more consistent with minor changes in the shape or microenvironment of the active site than with mutagenesis of a residue critical for catalysis. The structure of DHNO shows a water molecule within hydrogen-bonding distance of Lys348 (Figure 2); the K348M mutation could disrupt this interaction.

Among the other active-site variants, substitution of Glu350 has a much larger effect than the K348M change, with the E350Q substitution decreasing the k_{cat}/K_{amine} value ~200-fold.

The effect on the k_{red} value in this case is only ~6-fold, while the K_d value increases ~60-fold; therefore, the effect is mainly on binding. Surprisingly, changing this glutamate to alanine has a smaller effect than the more conservative replacement with glutamine. Indeed, the k_{red} value for the alanine variant is close to that of the wild-type enzyme, with almost the entire effect of the substitution being expressed in the K_d value; this clearly rules out a role for this residue as an active-site acid or base but is consistent with Glu350 providing a hydrogen bond critical for binding. The larger effect of the E350Q substitution may be due to the altered hydrogen bonding of the glutamine, consistent with the two positions of this residue seen in the crystal structure, resulting in an active site that is less reactive.

Glu352 has been proposed to have two different roles in the DHNO reaction. On the basis of the structure, Koetter and Shultz[10] proposed that this residue acts as an active-site base to

accept a proton from C3′ as the C2′–C3′ bond is oxidized; this proton would then be shuttled to Glu350 and thence to bulk solvent. The lack of a solvent isotope effect establishes that the nitrogen proton is not in flight during amine oxidation; thus, this role is unlikely. In contrast, Heath et al.[16] simply proposed an interaction between Glu350 and Glu352. The E352Q mutation results in a decrease in the k_{red} value that is ~30-fold greater than the decrease seen with the E350Q enzyme. This is not consistent with a minimalist role for Glu352 of properly positioning Glu350 for proper binding of the substrate. One possibility that is consistent with the data is that the negative charge of the Glu352 carboxylate acts to neutralize the positive charge on the nitrogen that develops as the substrate is oxidized by transfer of a hydride from C2′ to the flavin. The decrease in the k_{red} value for the E352Q enzyme of ~200-fold is consistent with a decrease in transition-state stabilization of 3–4 kcal/mol.

The k_{cat}/K_{amine}–pH profile with (*R*)-6-hydroxynicotine as the substrate (Figure 1A) is consistent with the need for with one critical group on the enzyme or substrate to be protonated and a separate group to be unprotonated for amine oxidation. With this substrate, the pK_a values are too close together to assign values to each, so that only their average value can be determined with confidence. The average of the two pK_a values increases 0.5 unit with (*R*)-6-hydroxynornicotine as the substrate. The pK_a of the amine nitrogen in this substrate (9.5) is 0.9 unit higher than that of the physiological substrate (8.6),[32] establishing that the pK_a of the substrate contributes to the k_{cat}/K_{amine}–pH profile. The pH independence of the k_{red} value with (*R*)-6-hydroxynicotine is consistent with productive binding requiring that both the substrate and the enzyme be properly protonated; consequently, the k_{cat}/K_{amine} profile reflects protonations involved in binding rather than catalysis. This conclusion is supported by the pH dependence of the K_d value. The data do not rule out the possibility that incorrectly protonated forms can bind, but incorrect protonation must decrease the level of binding by 2–3 orders of magnitude.

The effects of the substitutions of active-site residues on the pH profiles suggest that the pK_a values listed in Table 3 cannot be readily assigned to single residues. The lack of a change in the k_{cat}/K_{amine} profiles when Lys348 is replaced with methionine is consistent with the protonation state of this residue not being critical for binding or catalysis. This is consistent with the very small effect of this substitution on the other kinetic parameters. Substitution of either Glu350 or Glu352 does affect the k_{cat}/K_{amine}–pH profile, so that their protonation states do contribute. Replacement of Glu350 with either glutamine or alanine increases the value of pK_2 to ~9.7. While this suggests that the basic pK_a value of ~8 seen in the profile for the wild-type enzyme can be assigned to this residue, this is exceptionally high for a glutamate. In the pH profile for the E352Q variant, both pK_a values are significantly altered; this is not consistent with this residue being solely responsible for a single pK_a in the profile. Moreover, the upper pK_a shows an increase to ~10 similar to that seen upon substituting Glu350, confirming that Glu350 is not solely responsible for the higher pK_a in the profile for the wild-type enzyme. The protonation state of the substrate also contributes to the pH profile, because the basic pK_a value is higher with 6-hydroxynornicotine, but none of the k_{cat}/K_{amine}–pH profiles show clear evidence for a pK_a value of 8.5 for a group that must be unprotonated. It is thus likely that the pK_a values in the these profiles reflect a combination of the substrate pK_a and those arising from multiple active-site residues. Figure 2 shows

hydrogen bond interactions in the active site of DHNO that involve Lys348, Glu350, or Glu352. Both carboxylate oxygens of Glu352 are within hydrogen bond distance (≤3.0 Å) of multiple moieties, including water molecules. Given the central role of this residue in this network, it is not surprising that its substitution has such a large effect.

CONCLUSIONS

The results presented here are consistent with the mechanism of amine oxidation by DHNO being the same as that of other amine-oxidizing flavoproteins, hydride transfer from the neutral amine (Scheme 4) rather than a mechanism involving a quinone methide. Over the pH range examined here, substrate binding requires that the amine substrate be neutral and that active-site residues be properly protonated. A hydrogen-bonding network in the active site provides the environment for stabilizing the positive charge that develops on the substrate during the reaction. Glu352 plays a key role in this network.

Supplementary Material

Refer to Web version on PubMed Central for supplementary material.

Funding

This work was supported in part by grants from the National Institutes of Health (R01GM058698) and the Welch Foundation (AQ-1245).

ABBREVIATIONS

DHNO	D-6-hydroxynicotine oxidase
VAO/PCMH	vanillyl oxidase/*p*-cresol methylhydroxylase

REFERENCES

(1). Brandsch R (2006) Microbiology and biochemistry of nicotine degradation. Appl. Microbiol. Biotechnol 69, 493–498. [PubMed: 16333621]

(2). Fitzpatrick PF (2018) The enzymes of microbial nicotine metabolism. Beilstein J. Org. Chem 14, 2295–2307. [PubMed: 30202483]

(3). Tang H, Wang L, Wang W, Yu H, Zhang K, Yao Y, and Xu P (2013) Systematic unraveling of the unsolved pathway of nicotine degradation in Pseudomonas. PLoS Genet 9, No. e1003923. [PubMed: 24204321]

(4). Wang SN, Liu Z, Tang HZ, Meng J, and Xu P (2007) Characterization of environmentally friendly nicotine degradation by Pseudomonas putida biotype A strain S16. Microbiology 153, 1556–1565. [PubMed: 17464070]

(5). Tararina MA, Janda KD, and Allen KN (2016) Structural analysis provides mechanistic insight into nicotine oxidoreductase from Pseudomonas putida. Biochemistry 55, 6595–6598. [PubMed: 27933790]

(6). Schenk S, Hoelz A, Krauss B, and Decker K (1998) Gene structures and properties of enzymes of the plasmid-encoded nicotine catabolism of Arthrobacter nicotinovorans. J. Mol. Biol 284, 1323–1339. [PubMed: 9878353]

(7). Grether-Beck S, Igloi GL, Pust S, Schilz E, Decker K, and Brandsch R (1994) Structural analysis and molybdenum-dependent expression of the pAO1-encoded nicotine dehydrogenase genes of Arthrobacter nicotinovorans. Mol. Microbiol 13, 929–936. [PubMed: 7815950]

(8). Decker K, and Bleeg H (1965) Induction and purification of stereospecific nicotine oxidizing enzymes from Arthrobacter oxidans. Biochim. Biophys. Acta, Enzymol. Biol. Oxid 105, 313–324.

(9). Decker K, and Dai VD (1967) Mechanism and specificity of L-and D-6-hydroxynicotine oxidase. Eur. J. Biochem 3, 132–138. [PubMed: 4965794]

(10). Koetter JWA, and Schulz GE (2005) Crystal structure of 6-hydroxy-D-nicotine oxidase from Arthrobacter nicotinovorans. J. Mol. Biol 352, 418–428. [PubMed: 16095622]

(11). Kachalova GS, Bourenkov GP, Mengesdorf T, Schenk S, Maun HR, Burghammer M, Riekel C, Decker K, and Bartunik HD (2010) Crystal structure analysis of free and substrate-bound 6-hydroxy-L-nicotine oxidase from Arthrobacter nicotinovorans. J. Mol. Biol 396, 785–799. [PubMed: 20006620]

(12). Gaweska H, and Fitzpatrick PF (2011) Structures and mechanism of the monoamine oxidase family. Biomol. Concepts 2, 365–377. [PubMed: 22022344]

(13). Ewing TA, Fraaije MW, Mattevi A, and Van Berkel WJH (2017) The VAO/PCMH flavoprotein family. Arch. Biochem. Biophys 632, 104–117. [PubMed: 28669855]

(14). Gries FA, Decker K, and Bruehmueller M (1961) Decomposition of nicotine by bacterial enzymes. V. The oxidation of L-6-hydroxynicotine to γ-methylaminopropyl 6-hydroxy-3-pyridyl ketone. Hoppe-Seyler's Z. Physiol. Chem 325, 229–241. [PubMed: 13901804]

(15). Fraaije MW, and Van Berkel WJH (1997) Catalytic mechanism of the oxidative demethylation of 4-(methoxymethyl)-phenol by vanillyl-alcohol oxidase: Evidence for formation of a pquinone methide intermediate. J. Biol. Chem 272, 18111–18116. [PubMed: 9218444]

(16). Heath RS, Pontini M, Bechi B, and Turner NJ (2014) Development of an R-selective amine oxidase with broad substrate specificity and high enantioselectivity. ChemCatChem 6, 996–1002.

(17). Fitzpatrick PF, Chadegani F, Zhang S, Roberts KM, and Hinck CS (2016) Mechanism of the flavoprotein L-hydroxynicotine oxidase: kinetic mechanism, substrate specificity, reaction product, and roles of active-site residues. Biochemistry 55, 697–703. [PubMed: 26744768]

(18). Denu JM, and Fitzpatrick PF (1992) pH and kinetic isotope effects on the reductive half-reaction of D-amino acid oxidase. Biochemistry 31, 8207–8215. [PubMed: 1356021]

(19). Strickland S, Palmer G, and Massey V (1975) Determination of dissociation constants and specific rate constants of enzyme-substrate (or protein-ligand) interactions from rapid reaction kinetic data. J. Biol. Chem 250, 4048–4052. [PubMed: 1126943]

(20). Palmer G, and Massey V (1968) Mechanisms of flavoprotein catalysis. In Biological Oxidation (Singer TP, Ed.) pp 263–300, John Wiley and Sons, New York.

(21). Fitzpatrick PF (2010) Oxidation of amines by flavoproteins. Arch. Biochem. Biophys 493, 13–25. [PubMed: 19651103]

(22). Adachi MS, Juarez PR, and Fitzpatrick PF (2010) Mechanistic studies of human spermine oxidase: Kinetic mechanism and pH effects. Biochemistry 49, 386–392. [PubMed: 20000632]

(23). Gordon A, and Katritzky AR (1968) A quantitative relation between heteroaromatic tautomeric equilibrium constants and solvent polarity. Tetrahedron Lett 9, 2767–2770.

(24). Fraaije MW, Veeger C, and Van Berkel WJH (1995) Substrate specificity of flavin-dependent vanillyl-alcohol oxidase from Penicillium simplicissimum: Evidence for the production of 4-hydroxycinnamyl alcohols from 4-allylphenols. Eur. J. Biochem 234, 271–277. [PubMed: 8529652]

(25). Carlson JC, Li S, Gunatilleke SS, Anzai Y, Burr DA, Podust LM, and Sherman DH (2011) Tirandamycin biosynthesis is mediated by co-dependent oxidative enzymes. Nat. Chem 3, 628–633. [PubMed: 21778983]

(26). Fitzpatrick PF (2015) Combining solvent isotope effects with substrate isotope effects in mechanistic studies of alcohol and amine oxidation by enzymes. Biochim. Biophys. Acta, Proteins Proteomics 1854, 1746–1755.

(27). Sobrado P, and Fitzpatrick PF (2003) Solvent and primary deuterium isotope effects show that lactate CH and OH bond cleavages are concerted in Y254F flavocytochrome b_2, consistent with a hydride transfer mechanism. Biochemistry 42, 15208–15214. [PubMed: 14690431]

(28). Gadda G (2008) Hydride transfer made easy in the reaction of alcohol oxidation catalyzed by flavin-dependent oxidases. Biochemistry 47, 13745–13753. [PubMed: 19053234]

(29). Menon V, Hsieh C-T, and Fitzpatrick PF (1995) Substituted alcohols as mechanistic probes of alcohol oxidase. Bioorg. Chem 23, 42–53.

(30). Popelková H, Fraaije MW, Novák O, Frébortová J, Bilyeu KD, and Frébort I (2006) Kinetic and chemical analyses of the cytokinin dehydrogenase-catalysed reaction: correlations with the crystal structure. Biochem. J 398, 113. [PubMed: 16686601]

(31). Cleland WW (2005) The use of isotope effects to determine enzyme mechanisms. Arch. Biochem. Biophys 433, 2–12. [PubMed: 15581561]

(32). Fitzpatrick PF, Chadegani F, Zhang S, and Dougherty V (2017) Mechanism of flavoprotein L-6-hydroxynicotine oxidase: pH and solvent isotope effects and identification of key active site residues. Biochemistry 56, 869–875. [PubMed: 28080034]

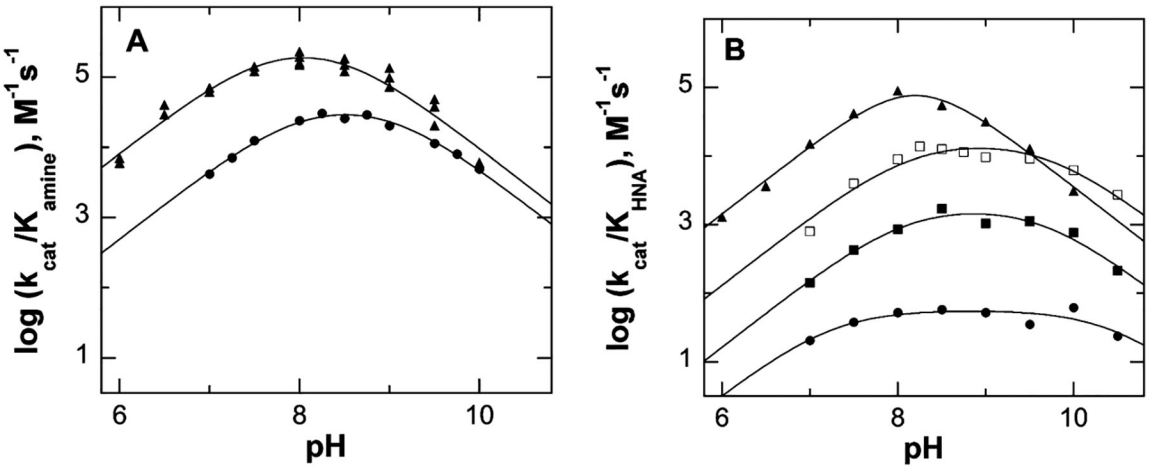

Figure 1.

Effect of pH on the k_{cat}/K_{amine} values for (A) wild-type DHNO with (*R*)-6-hydroxynicotine (▲) or (*R*)-6-hydroxynornicotine (●) as the substrate and (B) K348M (▲), E350Q (■), E350A (□), and E352Q (●) DHNO with (*R*)-6-hydroxynicotine as the substrate. The lines are from fits to eq 3.

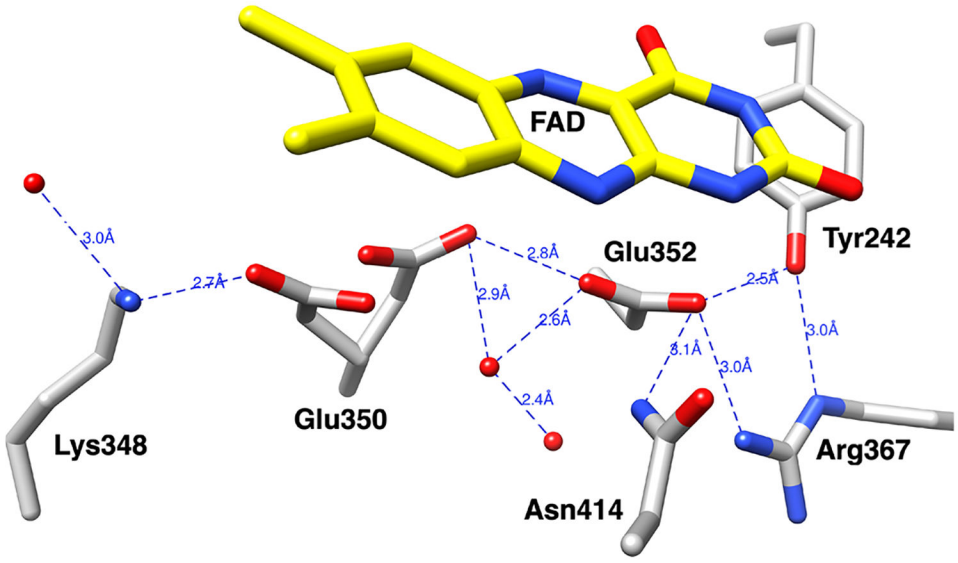

Figure 2.

Hydrogen bond interactions in the active site of DHNO (from Protein Data Bank entry 2BVF). Both orientations of Glu350 are shown.

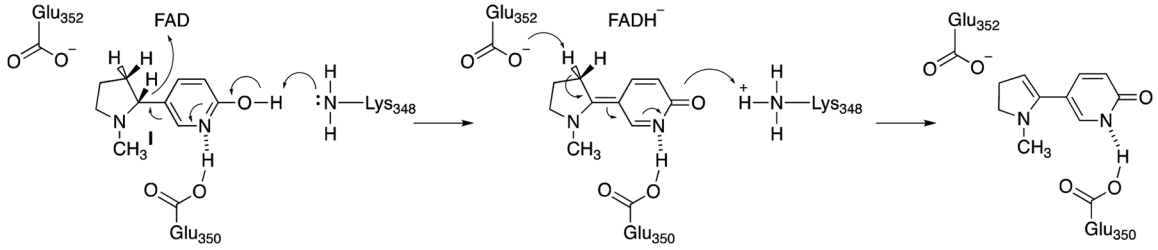

Scheme 1.
Proposed Mechanism for DHNO[10]

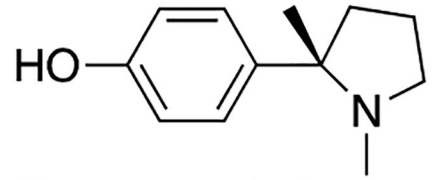

(R)-4-(1-methyl pyrrolidine-2-yl)phenol

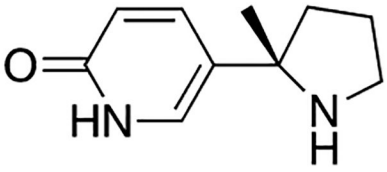

(R)-6-hydroxynornicotine

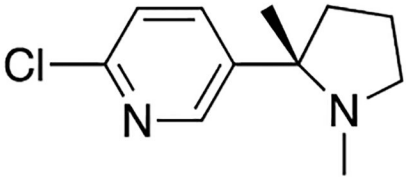

(R)-6-chloronicotine

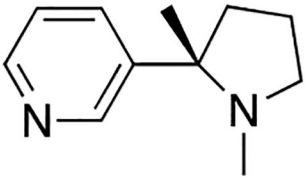

(R)-nicotine

Scheme 2.
Alternate Substrates for DHNO

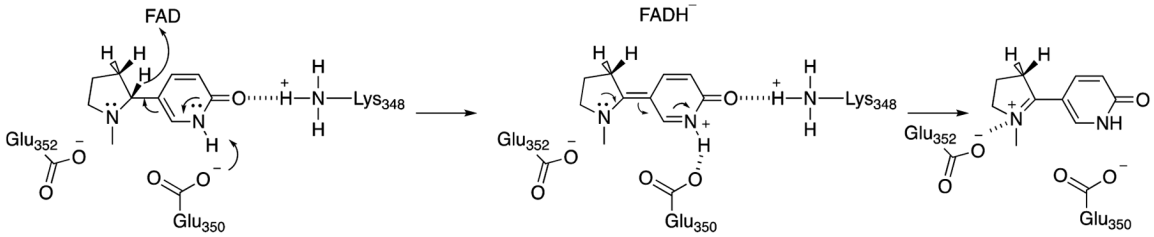

Scheme 3.

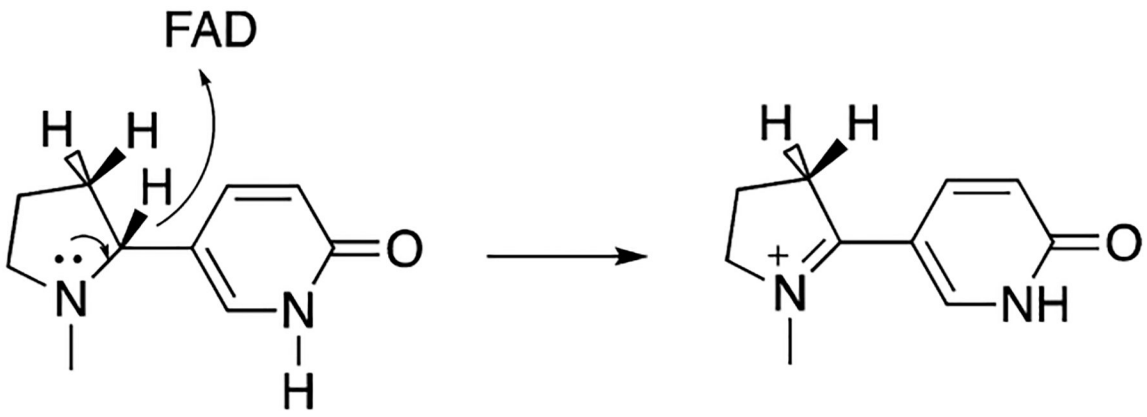

Scheme 4.

Table 1.

Steady-State Kinetic Parameters for Wild-Type and Mutant D-6-Hydroxynicotine oxidase[a]

enzyme	k_{cat} (s^{-1})	k_{cat}/K_{amine} ($mM^{-1}\ s^{-1}$)	K_{amine} (mM)	$k_{cat}/K_{O_2}\left(mM^{-1}\ s^{-1}\right)$	K_{O_2}(mM)
			(*R*)-6-Hydroxynicotine		
wild-type	77 ± 24[b]	380 ± 52[c]	0.20 ± 0.03	16 ± 1[b]	4.7 ± 1.7[b]
	8.7 ± 0.6[c]		0.023 ± 0.004[c]		
K348M	46 ± 7[b]	144 ± 4[c]	0.32 ± 0.06	39 ± 4[b]	1.2 ± 0.3[b]
	12 ± 1[c]		0.080 ± 0.015[c]		
E350Q	9.3 ± 1.8[b]	1.7 ± 0.2[c]	5.5 ± 1.0	21 ± 6[b]	0.43 ± 0.19[b]
	5.6 ± 0.7[c]		3.3 ± 0.8[c]		
E350A	20 ± 2[b]	17.8 ± 1.2[c]	1.12 ± 0.14	11.5 ± 0.5[b]	1.8 ± 0.2[b]
	3.5 ± 0.2[c]		0.78 ± 0.09[c]		
E352Q	0.63 ± 0.03	0.10 ± 0.01[c]	6.0 ± 0.5	3.2 ± 0.4[b]	0.20 ± 0.03[b]
	0.76 ± 0.12[c]		7.2 ± 1.7[c]		
			(*R*)-6-Hydroxynomicotine		
wild-type[c]	8.1 ± 0.5	24 ± 3	0.34 ± 0.06		
K348M[c]	5.4 ± 0.1	6.5 ± 0.3	0.83 ± 0.06		
			(*R*)-Nicotine		
wild-type[c]	0.26 ± 0.02	0.15 ± 0.01	0.84 ±0.12		
			(*R*)-6-Chloronicotine		
wild-type[c]	0.85 ± 0.04	4.0 ± 0.4	0.21 ± 0.03		
			(*R*)-4-(1-Methylpyrrolidine-2-yl) phenol		
wild-type[c]	1.5 ± 0.1	4.0 ± 0.2	0.36 ± 0.03		

[a]Conditions: 0.1 M Na-HEPES (pH 8.0), 0.1 M NaCl, 25 °C.

[b]Determined at 1–4 mM amine by varying the concentration of oxygen.

[c]Determined at 250 μM O_2 by varying the concentration of the amine.

Table 2.

Rapid-Reaction Kinetic Parameters for Wild-Type and Mutant D-6-Hydroxynicotine Oxidase[a]

enzyme	k_{red} (s^{-1})	K_d (mM)
(*R*)-6-Hydroxynicotine		
wild-type	490 ± 20	0.35 ± 0.05
K348M	360 ± 30	1.1 ± 0.3
E350Q	81 ± 15	21 ± 5
E350A	274 ± 10	9.0 ± 0.5
E352Q	2.6 ± 0.5	2.9 ± 1.3
(*R*)-6-Hydroxynomicotine		
wild-type	130 ± 3	2.0 ± 0.1
(R)-Nicotine		
wild-type	0.59 ± 0.02	0.032 ± 0.005
(*R*)-6-Chloronicotine		
wild-type	2.2 ± 0.1	0.35 ± 0.06
(*R*)-4-(l-Methylpyrrolidine-2-yl)phenol		
wild-type[a]	2.83 ± 0.02	0.22 ± 0.01

[a]Conditions: 0.1 M Na-HEPES (pH 8.0), 0.1 M NaCl, 25 °C.

Table 3.

pK_a Values from k_{cat}/K_m Profiles for D-6-Hydroxynicotine Oxidase[a]

enzyme	pK_1[b]	pK_2[b]
(*R*)-6-Hydroxynicotine		
wild-type	7.5 ±0.1	8.5 ± 0.1
	(8.05 ± 0.04)	(8.05 ± 0.04)
K348M	8.4 ± 0.3	8.0 ± 0.3
	(8.20 ± 0.03)	(8.20 ± 0.03)
E350Q	8.1 ± 0.1	9.7 ± 0.1
E350A	8.1 ± 0.2	9.8 ± 0.2
E352Q	7.2 ± 0.2	10.4 ± 0.2
(*R*)-6-Hydroxynomicotine		
wild-type	8.0 ± 0.1	9.1 ± 0.1
K348M	8.2 ±0.1	8.9 ±0.1

[a] Conditions: 250 μM oxygen, 25 °C.

[b] Calculated using eq 3; values in parentheses were calculated using eq 3 with $K_1 = K_2$.